JOURNAL OF MAGNETIC RESONANCE **133,** 232–235 (1998)
ARTICLE NO. MN981454

# Detection of Phosphomonoester Signals in Proton-Decoupled $^{31}$P NMR Spectra of the Myocardium of Patients with Myocardial Hypertrophy

Wulf-Ingo Jung,*,‡ Ludger Sieverding,† Johannes Breuer,† Oliver Schmidt,*,‡ Stefan Widmaier,*,‡ Michael Bunse,*,‡ Franz van Erckelens,* Jürgen Apitz,† Guenther J. Dietze,‡ and Otto Lutz*

**Physikalisches Institut, and †Division of Pediatric Cardiology, University of Tübingen, 72076 Tübingen, Germany; and ‡Hypertension and Diabetes Research Unit, Max Grundig Clinic, 77815 Bühl, Germany*

Received October 9, 1997

**Proton-decoupled $^{31}$P NMR spectroscopy at 1.5 T of the anterior left ventricular myocardium was used to monitor myocardial phosphate metabolism in asymptomatic patients with hypertrophic cardiomyopathy (HCM, $n = 14$) and aortic stenosis (AS, $n = 12$). In addition to the well-known phosphorus signals a phosphomonoester (PME) signal was detected at about 6.9 ppm in 7 HCM and 2 AS patients. This signal was not observed in the spectra of normal controls ($n = 11$). We suggest that in spectra of patients with myocardial hypertrophy the presence of a PME signal reflects alterations in myocardial glucose metabolism.** 

*Key Words:* **$^{31}$P MRS; myocardial hypertrophy; phosphomonoesters; human.**

## INTRODUCTION

Multiple small areas of myocardial ischemia and increased myocardial glucose consumption that occur in hypertrophied myocardium are discussed (*1–8*). In patients with hypertrophic cardiomyopathy (HCM) or aortic stenosis (AS) such inhomogenous perfusion may be involved in the pathophysiology of arrhythmias which could cause sudden unexpected death in these patients (*8–11*). To investigate the link between a possible reduction in myocardial perfusion and alterations in myocardial glucose metabolism may therefore be helpful in identifying patients at risk or those who should be surgically treated to relieve left ventricular outflow tract obstruction (LVOTO).

Expected changes in myocardial phosphate metabolism can be monitored by $^{31}$P NMR spectroscopy allowing the determination of intracellular pH ($pH_i$) (*12, 13*) and of high-energy phosphates (*14, 15*). This method has already been employed to examine patients with various heart diseases using the phosphocreatine (PCr) to adenosinetriphosphate (ATP) ratio (*16–23*) or the PCr to inorganic phosphate ($P_i$) ratio (*16, 21*) as a marker of the metabolic state of the myocardium.

In the present study on asymptomatic patients, proton-decoupled localized $^{31}$P NMR spectroscopy of small volume elements revealed in addition to these well-known phosphorus signals a PME signal at about 6.9 ppm in 9 out of 26 patients with myocardial hypertrophy. The signal which originated from myocardium was not observed in spectra of normal controls. This PME signal most likely reflects alterations in myocardial glucose metabolism.

## METHODS

We examined 26 young asymptomatic patients with HCM ($n = 14$, 5 female, mean age 16 ± 7 y) and AS ($n = 12$, 6 female, mean age 16 ± 4 y), as well as normal volunteers ($n = 11$, 1 female, mean age 27 ± 3 y). None of the patients showed symptoms of heart failure. The examinations were carried out on a 1.5-T whole-body imager (Siemens, Erlangen, Germany) with $^{31}$P and $^{1}$H Larmor frequencies of 25.74 and 63.60 MHz, respectively. The imager was equipped with a second RF channel for proton decoupling. Transmission and reception were performed with a 100-mm-diameter double-resonant single-turn surface coil with the decoupling frequency set to the Larmor frequency of the water protons.

The patients were positioned prone to the surface coil such that the anterior region of the heart was located just above the center of the surface coil. Flow-rephased gradient echo proton images were acquired to control the position of the volume of interest. Subsequent nonlocalized ECG-gated shimming was performed on protons up to water linewidths between 13 and 25 Hz within about 5 min.

A two-dimensional ECG-gated phosphorus chemical-shift imaging sequence (CSI) in combination with axial slice-selective excitation, coronal slice selective chest muscle saturation, and WALTZ4 proton decoupling was used to perform a complete three-dimensional localization. This procedure was previously described in detail (*24*). The pulse angle in the coil center was set to 180° and the sequence was triggered to every heartbeat. The application of this sequence with 2048 acquisitions resulted in spectra out of $5 \times 2.5 \times 3$ cm$^3$ or 38 ml volume elements within measurement times of 25–35 min—see Fig. 1.



1090-7807/98 $25.00

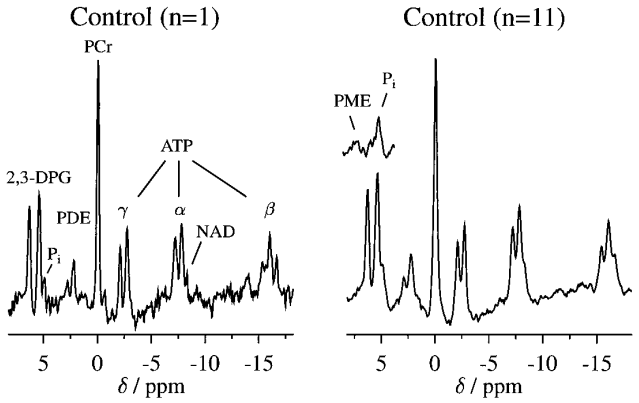


**FIG. 1.** Typical $^{31}$P NMR spectrum of the anterior left ventricular wall of a 25-year-old normal control (left, TR: 952 ms), and the average spectrum of the 11 spectra of all 11 normal controls (right, mean TR: 973 ms). The spectra are scaled for equal PCr peak height. The inset of the right spectrum shows a part of the spectrum after subtraction of the 2,3-DPG, PCr, and ATP signals obtained from the fit (see text).

Only one volume element of each subject's data set was chosen. This contained the apical part of the interventricular septum (IVS), and the anterior part of the left ventricular free wall located close to it (*24*). The signal of this volume element was zero filled to 4k, multiplied with a Gaussian function ($t_{1/2}$ = 150 ms, center at $t$ = 0), Fourier transformed, and phase corrected.

To focus on small signals in the phosphomonoester region of the spectra a time domain fit using VARPRO (*25*) and Gaussian model functions was carried out. The fit results for 2,3-diphosphoglycerate (2,3-DPG), PCr, and ATP were then subtracted from the spectra, leading to a simplified spectral pattern of the phosphomonoester region and a flattened baseline as shown, for example, in Fig. 2.

Due to the limited signal-to-noise ratio of the spectra of normal controls we performed a summation of all 11 individual spectra of the controls after normalizing them to equal PCr and setting the PCr to 0.00 ppm. The sum was then divided by 11, resulting in the average spectrum.

## RESULTS

Figure 1 shows a spectrum of a 25-year-old normal control and the average spectrum of all 11 normal controls. The signals were assigned as PME, 2,3-DPG; $P_i$, phosphodiesters (PDE); PCr, $\gamma$-, $\alpha$-, $\beta$-ATP, and nicotinamide adenine dinucleotide (NAD). The 2,3-DPG signals and a small part of PDE and ATP originate from blood in the left ventricular chamber. The inset shows the phosphomonoester region after subtracting from the average spectrum the great signals, especially 2,3-DPG (see Methods). The indication ''PME'' in the inset was assigned despite its very low signal-to-noise ratio even in the average spectrum of the 11 controls in order to provide a comparison to the spectra of the patients in Fig. 2.

Figure 2 shows individual spectra of HCM and AS patients together with their corresponding insets of the phosphomonoester region. In the bottom left spectrum of a HCM patient with a IVS of 43 mm no 2,3-DPG signal could be detected because the volume element was completely positioned within the myocardium. The subsequent subtraction was therefore carried out only with PCr and ATP in this case. The most prominent difference between these spectra and the control spectra in Fig. 1 is the presence of a clearly visible PME signal in the four patient spectra. This can be derived from three of the four presented cases directly from the measured spectra. Only in the top right spectrum is a more clear presentation obtained in the inset. The 2,3-DPG signal of blood in the HCM spectra is small (Fig. 2, top left) or even below the threshold of detection (Fig. 2, bottom left) due to the extent of hypertrophy. In addition, the HCM spectra and to a lesser degree also the AS spectra exhibited a higher signal-to-noise ratio due to the greater amount of tissue within the volume of interest.

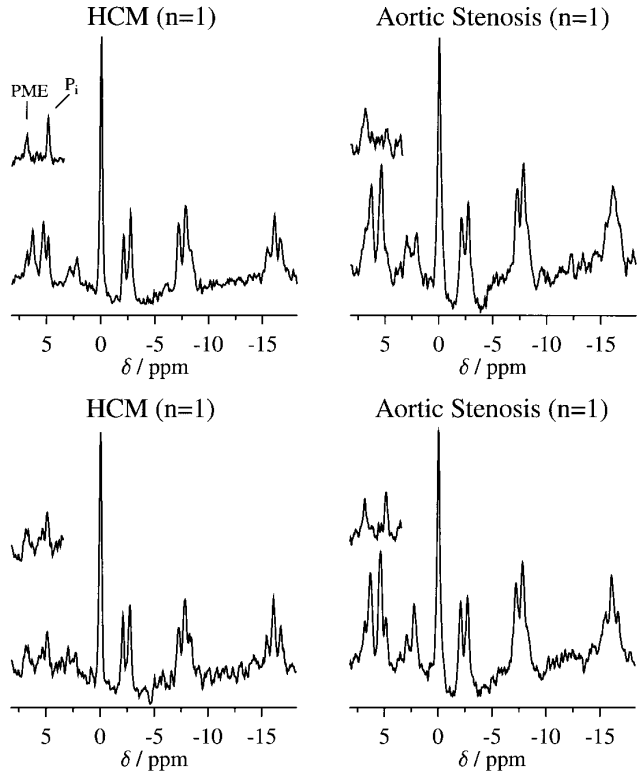


**FIG. 2.** $^{31}$P NMR spectra of the anterior left ventricular wall of two HCM (left) and two AS (right) patients. Top left: IVS: 37 mm, LVOTO: 32 mmHg; age: 10 y, sex: male; TR: 746 ms. Bottom left: IVS: 43 mm, LVOTO: none, age: 23 y, sex: female, TR: 1102 ms. Top right: IVS: 17 mm, LVOTO: 82 mm Hg, age 10 y, female, TR: 765 ms. Bottom right: IVS: 18 mm, LVOTO: 65 mm Hg, age 11, sex: male, TR: 1120 ms. Only a subtraction of PCr and ATP but no subtraction of 2,3-DPG was carried out for the inset of the bottom left spectrum. All these patient spectra exhibit a clearly detectable PME signal (see insets). See also legend to Fig. 1 and text.

## DISCUSSION

The patient spectra shown in Fig. 2 clearly revealed a PME signal at about 6.9 ppm close to the left shoulder of the 2,3-DPG signal of blood. To our knowledge, the presence of such a PME signal in human cardiac spectra has not been described so far. This PME signal was clearly visible in 7 out of 14 spectra of our patients with severe HCM and in 1 out of 12 patients with AS. In the case of one patient with AS and a less well resolved spectrum the PME signal was visible only as a pronounced left shoulder of 2,3-DPG and gained more clarity after subtracting the main strong signals (Fig. 2, top right). A possible PME signal could not be separated from noise in the remaining spectra of patients and controls. Only in the average spectrum of the 11 control spectra does a very small PME signal seem to be visible and it was tentatively assigned in the inset of Fig. 1.

In addition to the signals from myocardium, the spectra in Figs. 1 and 2 with the exception of Fig 2 bottom left also show signals from blood (*26*) in the left ventricular chamber: the 2,3-DPG signals and a greater part of PDE. In addition, a small amount of $P_i$ and a somewhat larger amount of ATP also originate from blood. The reason for the blood contamination in the spectra is the size and shape of the volume element which is necessary to end up with a satisfying signal-to-noise ratio. Thus, either the voxel has to be positioned partly in the chest muscle wall, which prevents contamination from blood signals but leads to contamination from skeletal muscle, or—as carried out here—the location of the voxel can be moved deeper into the heart such that no chest muscle signal contributes but blood contamination can occur. The 2,3-DPG signal can be used as a marker for the amount of blood contamination in the spectra. Since the spectrum of the HCM patient with severe hypertrophy, shown in the bottom left of Fig. 2, showed no detectable 2,3-DPG signal but a clearly visible PME signal, the PME signal could not originate from blood contamination. This fact was confirmed by a second spectrum of a HCM patient with clearly visible PME but undetectable 2,3-DPG signal (not shown).

To exclude contaminating signals from liver tissue a suitable transverse slice selection (*24*) was employed which ensured that liver tissue was not excited. Furthermore, artificial signals from the liver would contribute to both PME and PDE. The PDE signal, however, is smaller in the HCM spectra in Fig. 2 than in the control average spectrum, while the PME signal is greater. It is therefore unlikely that the greater PME signal originates from contaminating liver tissue. Moreover, contaminating signals from the liver would occur also in spectra of normal controls and thus would be visible as a PME signal, which is not the case.

It is therefore most likely that the PME signal originates from the myocardium. The evaluation of this signal might provide information about the activity of glucose metabolism because the PME signal is known to cover glycolytic intermediates and to a lesser degree also adenosinemonophosphate (AMP) (*27, 28*). Indeed, such alterations in myocardial glucose metabolism were found in myocardial hypertrophy in animals (*5–7*) and humans (*3, 4*). Smith *et al.* (*5*) detected in hypertrophied rat myocardium decreased oxidative phosphorylation and increased nonoxidative glucose metabolism. Anderson *et al.* (*6*) also reported that hypertrophied rat hearts have a greater potential for nonoxidative glycolytic metabolism leading to an increased by-product accumulation. Evidence for altered glucose metabolism is further provided by Kagaya *et al.* (*7*), who found increased uptake of labeled glucose and decreased extraction of free fatty acids in the hypertrophied rat myocardium induced by creation of aortic stenosis. In humans, PET studies of patients with HCM have been performed which support the hypothesis of a shift of cardiac metabolism toward glucose consumption (*3, 4*) showing heterogeneously elevated glucose retention in the myocardium.

Thus, the PME signal in the spectra of the patients presented in Fig. 2 most likely reflects alterations in myocardial glucose metabolism. Since PME was visible in only 7 out of 14 HCM patients and in 2 out of 12 AS patients, more examinations will now be necessary to illuminate its origin. It is known from animal studies (*27*) that the PME signal in rat heart covers glucose-6-phosphate, $\alpha$-glycerolphosphate, and further glycolytic intermediates and to a lesser degree also AMP; thus, a suitable model function for a fit of the PME signal is not available. This also explains why it is so difficult to provide here an exact chemical shift of PME. Moreover, neither $T_1$ relaxation nor the NOE enhancement of this signal group is known. Thus, considerable problems will have to be solved before a quantitative analysis is possible, especially in light of the exclusive visibility of PME in spectra of patients. Moreover, it remains unclear at the moment why not all patients exhibited a PME signal. This surprising fact is similar to findings in ischemic rat heart (*27*) where a PME signal was present only in those hearts which did not recover well after ischemia. Our patient group is at the moment too heterogeneous to allow formation and statistical evaluation of different subgroups which would eventually help to solve this question. Patients may, for example, be stratified according to age, degree of LVOTO, extent of myocardial hypertrophy, and genetic aspects. It will be interesting to see whether detection and evaluation of the PME signal in clinical cardiac spectroscopic investigations may help to increase the amount of information beyond that obtained by the PCr/ATP and $P_i$/PCr ratios frequently used.

## ACKNOWLEDGMENTS

Financial support by the Hans und Gertie-Fischer-Stiftung, the Deutsche Herzstiftung, the Alfried Krupp von Bohlen and Halbach-Stiftung, and the Fortüne program of the University of Tübingen is gratefully acknowledged. We thank Siemens Medizintechnik, Erlangen, for continuous support, and the members of the magnetic resonance imaging facility and of the Hypertension and Diabetes Research Unit of the Max Grundig Clinic for their help and advice.

## REFERENCES


1. P. T. O'Gara, R. O. Bonow, B. J. Maron, B. A. Damske, A. van Lingen, S. L. Bacharach, S. M. Larson, and S. E. Epstein, Myocardial perfusion abnormalities in patients with hypertrophic cardiomyopathy: Assessment with thallium-201 emission computed tomography, *Circulation* **76,** 1214–1223 (1987).
2. P. Camici, G. Chiaretti, R. Lorenzoni, R. C. Bellina, R. Gistri, G. Italiani, O. Parodi, P. A. Salvadori, N. Nista, L. Papi, and A. L'Abbate, Coronary vasodilatation is impaired in both hypertrophied and non-hypertrophied myocardium of patients with hypertrophic cardiomyopathy: A study with nitrogen-13 ammonia and positron tomography, *J. Am. Coll. Cardiol.* **17,** 879–886 (1991).
3. C. A. Nienaber, S. S. Gambhir, F. V. Mody, O. Ratib, S. C. Huang, M. E. Phelps, and H. R. Schelbert, Regional myocardial blood flow and glucose utilization in symptomatic patients with hypertrophic cardiomyopathy, *Circulation* **87,** 1580–1590 (1993).
4. P. Perrone-Filardi, S. L. Bacharach, V. Dilsizia, J. A. Panza, S. Maurera, and R. O. Bonow, Regional systolic function, myocardial blood flow and glucose uptake at rest in hypertrophic cardiomyopathy, *Am. J. Cardiol.* **72,** 199–204 (1993).
5. S. H. Smith, M. F. Kramer, I. Reis, S. P. Bishop, and J. S. Ingwall, Regional changes in creatine kinase and myocyte size in hypertensive and nonhypertensive cardiac hypertrophy, *Circ. Res.* **67,** 1334–1344 (1990).
6. P. G. Anderson, M. F. Allard, G. D. Thomas, S. P. Bishop, and S. B. Digerness, Increased ischemic injury but decreased hypoxic injury in hypertrophied rat hearts, *Circ. Res.* **67,** 948–959 (1990).
7. Y. Kagaya, Y. Kanno, D. Takeyama, N. Ishide, Y. Maruyama, T. Takahashi, Y. Ido, and T. Takishima, Effect of long-term pressure overload on regional myocardial glucose and free fatty acid uptake in rats, *Circulation* **81,** 1353–1361 (1990).
8. E. Braunwald, ''Heart Disease. A Textbook of Cardiovascular Medicine,'' 5th ed., Saunders, Philadelphia (1997).
9. W. J. McKenna and A. J. Camm, Sudden death in hypertrophic cardiomyopathy: Assessment of Patients at High Risk, *Circulation* **80,** 1489–1492 (1989).
10. L. A. Aron, H. L. Hertzenau, E. Z. Fisman, I. S. Nostrati, and J. J. Kellermann, Prognosis of non-obstructive hypertrophic cardiomyopathy, *Am. J. Cardiol.* **67,** 215–217 (1991).
11. Y. Drory, Y. Turetz, Y. Hiss, B. Lev, E. Z. Fisman, A. Pines, and M. R. Kramer, Sudden unexpected death in persons $<$40 years of age, *Am. J. Cardiol.* **68,** 1388–1392 (1991).
12. R. B. Moon and J. H. Richards, Determination of intracellular pH by $^{31}$P magnetic resonance, *J. Biol. Chem.* **25,** 7276–7278 (1973).
13. O. A. C. Petroff, J. W. Prichard, K. L. Behar, J. R. Alger, J. A. den Hollander, and R. G. Shulman, Cerebral intracellular pH by $^{31}$P nuclear magnetic resonance spectroscopy, *Neurology* **35,** 781–788 (1985).
14. S. Wray and P. S. Tofts, Direct in vivo measurement of absolute metabolite concentrations using $^{31}$P nuclear magnetic resonance spectroscopy, *Biochim. Biophys. Acta.* **886,** 399–405 (1986).
15. G. J. Kemp and G. K. Radda, Quantitative interpretation of bioenergetic data from $^{31}$P and $^{1}$H magnetic resonance spectroscopic studies of skeletal muscle: An analytical review, *Magn. Reson. Quart.* **10,** 43–63 (1994).
16. P. A. Bottomley, R. J. Herfkens, L. S. Smith, and T. M. Bashore, Altered phosphate metabolism in myocardial infarction: P-31 NMR spectroscopy, *Radiology* **165,** 703–707 (1987).
17. R. G. Weiss, P. A. Bottomley, C. J. Hardy, and G. Gerstenblith, Regional myocardial metabolism of high-energy phosphates during isometric exercise in patients with coronary artery disease, *N. Engl. J. Med.* **323,** 1593–1600 (1990).
18. S. Schaefer, J. R. Gober, G. G. Schwartz, D. B. Twieg, M. W. Weiner, and B. Massie, In vivo phosphorus-31 spectroscopic imaging in patients with global myocardial disease, *Am. J. Cardiol.* **65,** 1154–1161 (1990).
19. M. A. Conway, J. Allis, R. Ouwerkerk, T. Niioka, B. Rajagopalan, and G. K. Radda, Detection of low phosphocreatine to ATP ratio in failing hypertrophied human myocardium by $^{31}$P magnetic resonance spectroscopy, *Lancet* **338,** 973–976 (1991).
20. S. Neubauer, T. Krahe, R. Schindler, M. Horn, H. Hillenbrand, C. Entzeroth, H. Mader, E. P. Kromer, G. A. J. Riegger, K. Lackner, and G. Ertl, $^{31}$P magnetic resonance spectroscopy in dilated cardiomyopathy and coronary artery disease, *Circulation* **86,** 1810–1818 (1992).
21. A. de Roos, J. Doornbos, P. R. Luyten, L. J. M. P. Oosterwaal, E. E. van der Wall, and J. A. den Hollander, Cardiac metabolism in patients with dilated and hypertrophic cardiomyopathy: Assessment with proton-decoupled P-31 MR spectroscopy, *J. Magn. Reson. Imaging* **2,** 711–719 (1992).
22. T. Yabe, K. Mitsunami, M. Okada, S. Morikawa, T. Inubushi, and M. Kinoshita, Detection of myocardial ischemia by $^{31}$P magnetic resonance spectroscopy during handgrip exercise, *Circulation* **89,** 1709–1716 (1994).
23. T. Yabe, K. Mitsunami, M. Okada, T. Inubushi, and M. Kinoshita, Quantitative measurements of cardiac phosphorus metabolites in coronary artery disease by $^{31}$P magnetic resonance spectroscopy, *Circulation* **92,** 15–23 (1995).
24. W. I. Jung, S. Widmaier, U. Seeger, M. Bunse, A. Staubert, L. Sieverding, K. Straubinger, F. van Erckelens, F. Schick, G. Dietze, and O. Lutz, Phosphorus J-coupling constants of ATP in human myocardium and calf muscle, *J. Magn. Reson. B.* **110,** 39–46 (1996).
25. J. W. C. van der Veen, R. de Beer, P. R. Luyten, and D. van Ormondt, Accurate quantification of *in vivo* $^{31}$P NMR signals using the variable projection method and prior knowledge, *Magn. Reson. Med.* **6,** 92–98 (1988).
26. M. Horn, S. Neubauer, M. Bomhard, M. Kadgien, K. Schnackerz, and G. Ertl, $^{31}$P-NMR spectroscopy of human blood and serum: First results from volunteers and patients with congestive heart failure, diabetes mellitus and hyperlipidaemia, *MAGMA* **1,** 55–60 (1993).
27. F. M. H. Jeffrey, C. J. Storey, and C. R. Malloy, Predicting functional recovery from ischemia in the rat myocardium, *Basic Res. Cardiol.* **87,** 548–558 (1992).
28. S. Neubauer and J. S. Ingwall, Verapamil attenuates ATP depletion during hypoxia: $^{31}$P NMR studies of the isolated rat heart, *J. Mol. Cell. Cardiol.* **21,** 1163–1178 (1989).